

Design of Water Treatment Compressors Equipped with Active Magnetic Bearings

M. Antila, E. Lantto, J. Saari

Helsinki University of Technology, Laboratory of Electromechanics
Otakaari 5A, FIN-02150 Espoo, Finland

H. Esa, O. Lindgren, K. Säily

High Speed Tech Ltd.
Tekniikantie 4D, FIN-02150 Espoo, Finland

Abstract: High Speed Tech Ltd. has constructed a high-speed water treatment compressor. The rotational speed is 42 000 rpm and the power is 75 kW. In this paper, a part of the facts that have to be considered when designing a high-speed machine are treated. In addition, some measurement results from the type tests are presented.

1 Introduction

In high-speed technology, the drive machine, for example a compressor, and the electrical machine have a common rotor without a gearbox. Typically, the rotation speeds vary between 20 000-100 000 rpm and the machines may have power outputs up to several hundreds of kilowatts. Technical properties of high-speed technology result in economic benefits through long lifetime, maintenance-free systems, easy control, small size, a dramatic simplification of process concepts, reduced production and component costs and high efficiency. Long lifetime and maintenance-free systems can be achieved, because the technology uses only rotational movements, contactless oil-free bearings and seals. Systems become simpler because separate lubrication system is not needed. The small size enables the integration of the compressors straight to the process.

High-speed electric motors are widely applied in turbomachines such as pumps and compressors. The rotation speed is controlled by a frequency converter.

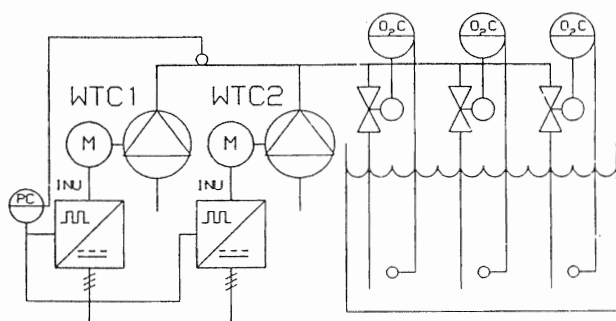


Fig 1. Application of high-speed compressors for water treatment.

The robust construction and contactless bearings enable much higher speeds than with conventional technology.

In Finland, our development has lately been focused on turbocompressors for industrial environment. One of the applications is the air compressor for sewage plants. The principle of this application is shown in Fig. 1. The oxygen level of the sewage pool is measured at several location and maintained homogeneous by controlling the air flow through corresponding valves. These valves are connected to the main pressure line. The main pressure is produced by several high-speed turbocompressors in parallel operation. The machine loads are determined by the pressure loss, i.e. the water level in the sewage pool. The flow is controlled by the rotational speed of the compressors.

2 Water treatment compressor

2.1 Construction of the machine

The construction of the air compressor is presented in Fig. 2. The machine consists of a compressor, an electric motor, active magnetic bearings and a cooling

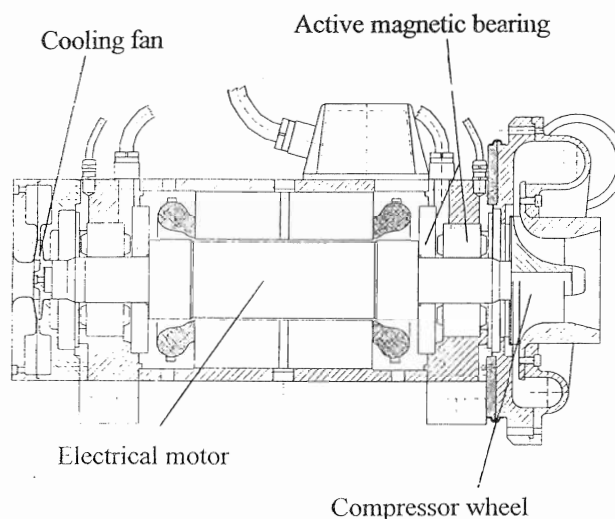


Fig 2. Construction of the water treatment compressor.

Electric motor

Inner diameter of stator [mm]	95
Core length [mm]	210
Weight of rotor [N]	200
Radial magnetic bearing	
Number of poles	8
Core length [mm]	45
Rotor diameter [mm]	54
Air gap [mm]	0.5

Table 1. Main parameters of the machine and bearings.

fan. The motor has a special solid-rotor construction which enables very high peripheral speeds (to 500 m/s). Moreover, the machine can be operated below the bending critical speeds. Because of the high power density, the machine is cooled by blowing air through the air gap and bearings. The cooling fan is connected directly to the motor shaft. The main parameters of the machine are presented in Table 1.

Fig. 3 presents the schematic performance map of a turbocompressor. The maximum rotational speed of the machine sets an upper bound to the pressure ratio and volume flow (and power) of the turbocompressor. Also, for a certain compressor the maximum efficiency area restricts the reasonable operation range of the machine. In normal operation, the efficiency of the compressor is above 70%. The surge and choke states of the compressor are prevented by the electronics.

2.2 Electric motor

The properties of the turbocompressor set a starting point for the design of an electrical motor. From the performance map, the shaft power and rotational speed ranges of the electrical motor are determined. Fig. 4 shows the operation range of the water treatment compressor.

Because of the wide operation range and the non-sinusoidal supply waveform, high-speed motors need careful electromagnetic and thermal designs. The motors constructed have been analyzed by finite-element [1] and thermal-network [2] programs.

The temperature-rise distribution in the electric machine is obtained by solving a two-dimensional thermal network. A computer program was developed for the solution of the thermal network. The input parameters for the program are the dimensions, rotation speed, electromagnetic losses and cooling method of the machine. The heat-transfer coefficients, friction losses, and cooling losses are determined in the program. The output from the thermal-network program is the temperature rise distribution as a function of the cooling gas flow rate.

Fig. 5 presents the calculated efficiency curves of the electrical motor. At high powers the efficiencies

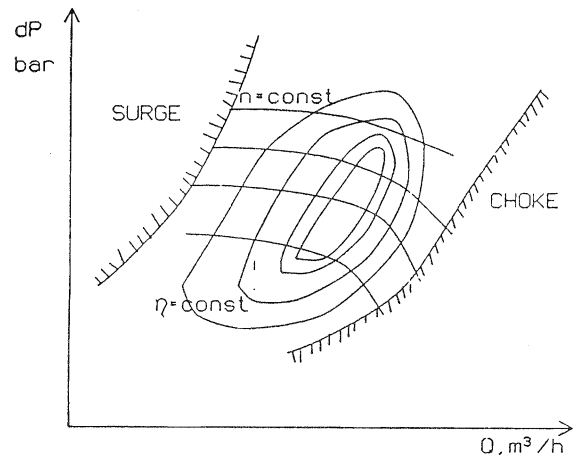


Fig 3. Schematic performance map of a turbocompressor.

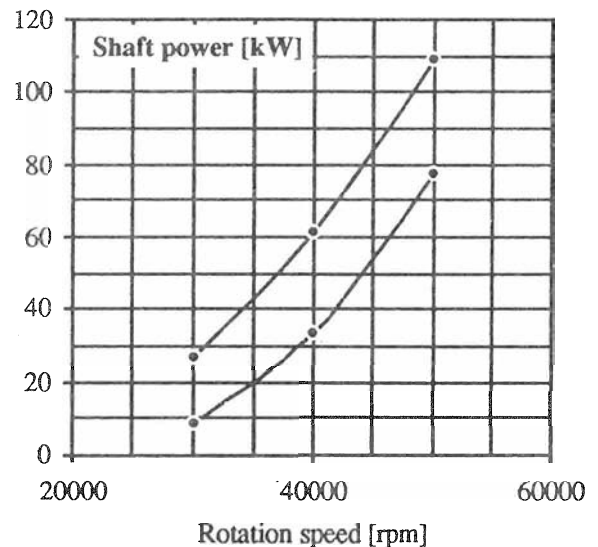


Fig 4. Operation area of the water treatment compressor.

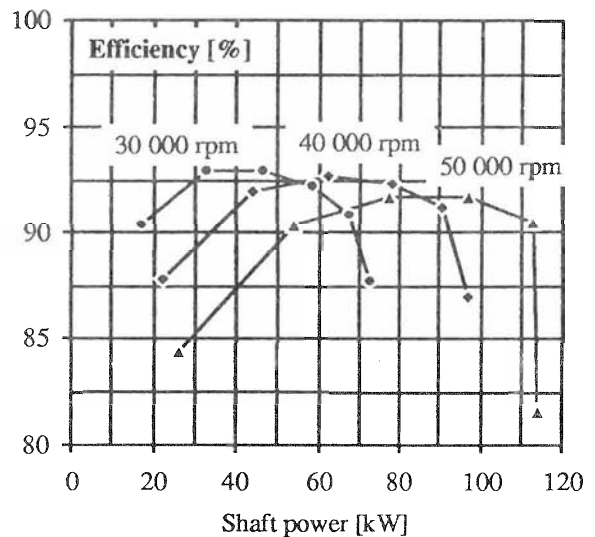


Fig 5. Efficiency of the electrical motor.

decrease dramatically, because of very high cooling losses. The optimal loads are 40 kW, 65 kW and 90 kW at speeds of 30 000, 40 000 and 50 000 rpm, respectively. The designed motor seems to fit the desired operation range. Loads above 100 kW are not recommended.

3 Active magnetic bearings

3.1 Magnetic bearing design

When designing active magnetic bearings for a high speed compressor there are certain performance requirements and boundary conditions to be met. The AMBs have to compensate the internal loads caused by the compressor wheel, electrical motor and the mass of the rotor. Also, external loads such as base vibrations have to be controlled. These requirements set a minimum to the air gap area of the radial bearing. On the other hand, the design of the bearing is restricted by the rotational speed of the machine. The tensile strength of silicon steel sheets corresponds to the maximum peripheral speed of about 200 m/s. Thus, the radius of the radial magnetic bearings is limited by the maximum rotational speed of the machine. The length of the bearing is chosen to satisfy the requirements of the air gap area.

Anyhow, there is an upper limit also to the length of the bearing. The most important factor influencing the bending critical speeds of the rotor is the solid shaft inside the steel sheets. Thus, by making the bearing longer the bending critical speeds are also lowered. In addition, the width of the steel sheet in the rotor is a design factor which affects to the properties of the radial bearing as well as to the bending critical speeds of the rotor. Thus, by changing the width of the steel sheet a designer can make a tradeoff between the bending critical speeds and the bearing force and losses.

Also, the winding restricts the design of the bearing. The current density in the coil should be low enough to keep the temperature at an acceptable level. Also, for series production it is favorable to keep the manufacturing of the coil and the bearing simple.

Thus, when designing an AMB system for a high-speed compressor several compromises have to be made. In order to find a successful and balanced design it is important to have reliable analysis tools. Also, when going for the series production of machines equipped with AMBs it is of primary importance to find the most critical factors of the design and manufacturing tolerances of the parameters. In this paper, the measurements done with the AMBs of the first machine of the pilot series are described. The main parameters of radial active magnetic bearings are shown in Table 1. The rotor disk of the axial bearing has the same diameter as the motor.

3.2 AMB control system design

Because the rotor is very symmetric, all the radial position regulators are similar. They are of PID-type. A sharp lowpass filter was set at 700 Hz to drop the bearing stiffness phase angle below -180° before the rotor bending frequencies. This trick will introduce slight damping to the first rotor bending mode and it will also effectively limit the controller bandwidth. A slight cross-coupling was done between the drive- and nondrive end controllers to increase the robustness of the control loop.

In the current control loop, a finite current feedback coefficient is used. This was chosen to be high enough so that the current control loop is fast enough in all the inductance variations, but not too fast. Too fast current control causes only noise and problems with power amplifier saturation.

The gain of the control loop was tuned high enough so that the controller can sustain good dynamic properties with all the airgap variations. Also, it was a demand that the bearing stiffness is high enough to compensate the dynamic disturbance forces caused by electrical motor and compressor surge. The electric motor causes remarkable forces at low speeds. On the other hand, it was carefully analyzed that the controller gain is not unnecessarily high. A high controller gain (and bearing stiffness) may lead to problems with foundation resonances.

There is some potential sources for parameter variations in series production. First, it is supposed that the electronics can be copied with sufficient accuracy, so that they can be considered identical. The airgaps in the bearing magnets vary due to manufacturing tolerances and thermal enlargements. The rotor position between the magnets will vary. These variations will change the bearing parameters (inductance, force-current factor and the destabilizing spring). The airgap variations and other factors in the displacement sensor will change the displacement sensor sensitivity. The goal of the controller design was to achieve sufficient robustness, so that when normal machine building tolerances are used in series production, no individual tuning is needed in series production. In the simulations, the airgaps were allowed to vary twice the tolerance limits and the thermal enlargements were estimated upwards. According to simulations, the bearings should work well through all these variations. In practice, we tested the controller by changing the position sensor sensitivity from its nominal value 1 to 0.5 and 1.8 in every channels (also so that one channel 0.5, others 1.8). The bearings sustained good dynamic properties with this high sensitivity variations and also they could produce the nominal force without vibrations.

The power amplifier can tolerate about 10 μm position vibration at 700 Hz without saturation. In practice, the vibration amplitudes remained below that

in all the machines of the pilot series. If the vibrations would be too high (for example the rotor starts bending already at 700 Hz) then an adaptive unbalance compensator is used.

According to tests, the AMB is robust enough for series production. Actually, we had to leave only one tunable parameter to the electronics. This parameter is the axial position reference. This was left in the electronics, because the efficiency of the compressor depends on the clearance between spiral base and the compressor wheel and this clearance needs to be adjusted.

3.3 Force measurements

In the force measurements, a pulley system was attached to one end of the shaft. A strain gauge was included in the pulley system to measure the applied load. The accuracy of the force measurement was $0.5\% \mp 2 \text{ N}$. The applied force at the bearing position was then calculated and the effect of the mass of the rotor was reduced in order to solve the magnetic bearing force. The load was applied diagonally between the coordinate axes. The bearing currents were measured with separate shunt resistors and voltage meters.

The force of the radial magnetic bearing was calculated from the finite element solution of the field equation by the method based on Maxwell's stress tensor. In Fig. 6 the calculated and measured force and control current characteristics of a radial bearing are compared. The agreement is found to be good with a maximum relative error less than ten percent in the measurement range. The largest deviations between calculated and measured forces are in the nonlinear region. This may be due to inaccurate material data.

The measurement of the axial bearing were done with the same measurement setup. In the axial bearing measurements, the maximum force upwards was applied to the rotor and then gradually removed until the only component acting to the axial bearing was the mass of the rotor. Then the applied force was gradually

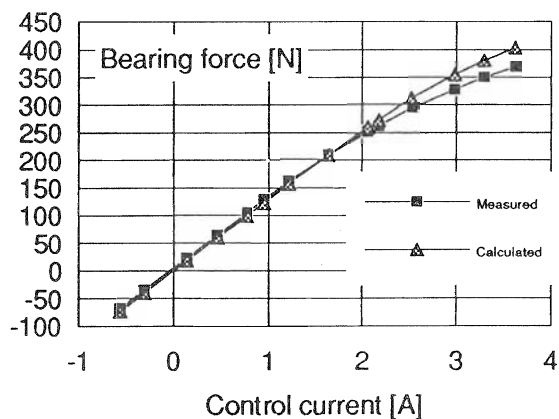


Fig 6. Force and control current characteristics of the radial bearing. The bias-current is 2.0 A.

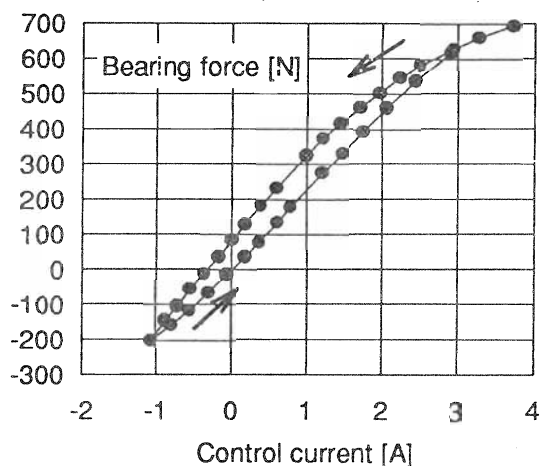


Fig 7. Force and control current characteristics of the axial bearing. The bias-current is 3.0 A.

increased up to the maximum load. Thus, a part of the hysteresis loop was measured. In Fig. 7, the force and control current characteristics of the axial bearing are shown. The hysteresis of the magnetic circuit can be clearly seen from Fig 7. The hysteresis together with the eddy-current effects make the modeling of the axial bearing a complicated task and a proper linearised model is difficult to find.

3.4 Measurement of the forces of the compressor wheel

A theoretical analysis of the forces of a compressor is a difficult task. Anyhow, some estimations of the forces can be done. In order to verify the design of the high-speed machine and its bearings, the forces of the compressor had to be measured. The forces were measured with the active magnetic bearings. The forces were measured with speeds between 24 000 and 42 000 rpm, mass flows between 0.191 and 0.824 kg/s and pressure ratios between 1.1 and 1.65. The error of the measured forces due to the hysteresis were $\pm 30 \text{ N}$ in the axial direction and $\pm 5 \text{ N}$ in the radial direction. In the measurements, the inlet pressure of the compressor was controlled by a throttle valve and the outlet was led to atmospheric pressure. Thus, the measurement set up was inversed compared to the actual operation of the water treatment compressor.

Fig. 8 represents the axial and radial forces of the compressor. The axial force is mainly determined by the pressure ratio of an operation point. By a proper design of labyrinth seals, a designer can control the axial forces. The measured axial forces are quite high compared with the measured load capacity of the axial bearing. The reason for this is the inversed setup of the compressor, which considerably increased the axial forces. In the actual application, the axial forces are negligible.

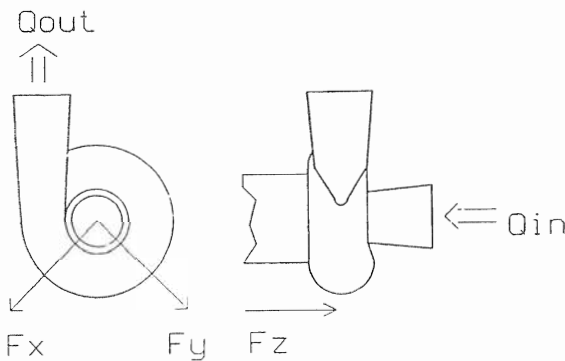
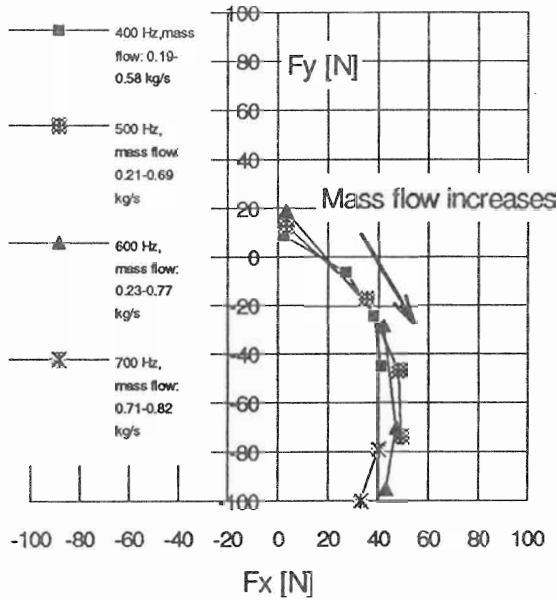
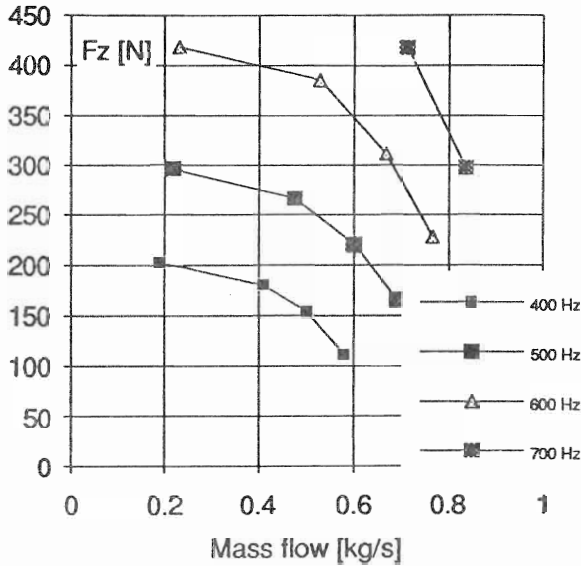


Fig 8. Axial and radial forces of the compressor and the corresponding coordinate system.

The radial forces increased with the mass flow and are fairly independent of the rotational speed. The maximum radial forces in one coordinate direction is about 100 N. This is well below of the load capacity of the radial bearing. Also, because the forces of the electric motor are largest at quite low frequencies [3], the load capacity of the radial bearings is sufficient.

3.4 Measurement of the Campbell diagram

The water treatment compressor is operated at speeds below the first bending critical speed. Thus, a reliable analysis tool of the rotor dynamics is a key factor when designing high-speed machines. Also, when designing the controller of AMB the elastic rotor vibration modes have to be considered. The rotor dynamics are modeled with a finite-element method (FEM) based on the Timoshenko beam theory [4].

The splitting of the rotor bending modes into forward and backward modes was measured. The zero-speed eigenfrequencies were measured before (and they agreed with the predictions), but this measurement was made in order to test the assumptions made in the rotordynamic modelling. Electric noise (power concentrated at the bending frequencies) was added to the output of the controller, and the spectrum of the rotor vibration was measured. From this spectrum, the eigenfrequencies were detected. The measured eigenfrequencies are plotted with the predicted eigenfrequencies in Fig. 9. This measurement confirmed that the beam FEM used for modeling the elastic rotor dynamics is accurate enough in this type of rotor. The first bending critical speed of the water treatment compressor is about 1000 Hz, so the marginal at maximum speed is 30 %. This should be enough. In the design stage, the rotor bending frequencies are also checked with a three dimensional FEM program.

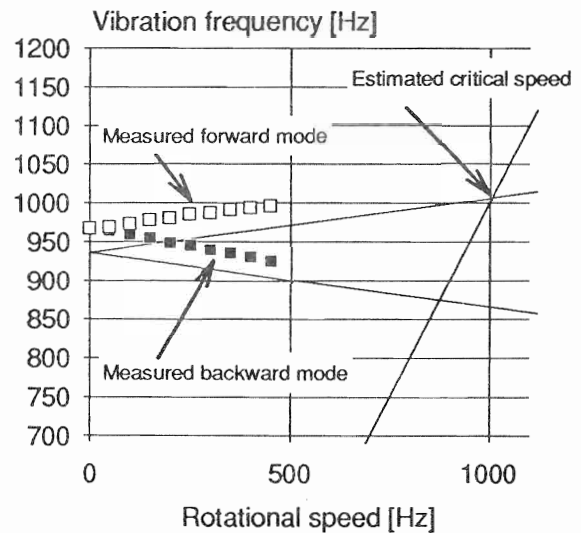


Fig 9. The measured and estimated Campbell diagram of the water treatment compressor.

3.5 Measurement of the windage losses and magnetic bearing losses

In this section, we are dealing with losses which affect to the shaft power of the machine. In a high-speed machine, friction losses are a major loss component. Together with the cooling loss they could cause 50 % of the total losses. So, in order to be able to estimate the efficiency of the electrical machine accurately, it is important to estimate the friction losses and the bearing losses. The friction losses in the airgaps can be estimated by the equations for rotating cylinders in enclosures or in free space. However, these equations are for smooth surfaces and in a high-speed machine the surfaces are not aerodynamically smooth. Thus, the estimation may not be exactly valid. Also, the losses in the magnetic bearings are difficult to estimate.

In order to separate the electromagnetic bearing losses and friction losses, the machine was rotated both in the atmospheric pressure and in the vacuum. The machine was rotated without the compressor wheel. From the deceleration of the machine the friction and bearing losses can be calculated. At first, to get an estimation of the losses of the axial bearing, the machine was rotated in vacuum with a bias current of 3.0 A. Then the bias current was raised to 4.0 A, which increased the square of the flux density approximately two times. Then the increase of losses were calculated. As the electromagnetic losses are proportional to the square of the flux density, it was estimated that the axial bearing at bias current of 3.0 A has losses 10 W. Fig. 10 represents the comparison between friction the losses and the electromagnetic losses of the radial bearings.

As can be seen, the friction losses are about ten times higher than the electromagnetic losses of the radial bearings. The axial bearings losses are about 5 % of the radial bearing losses. Thus, it is of major importance to be able to estimate the friction losses in

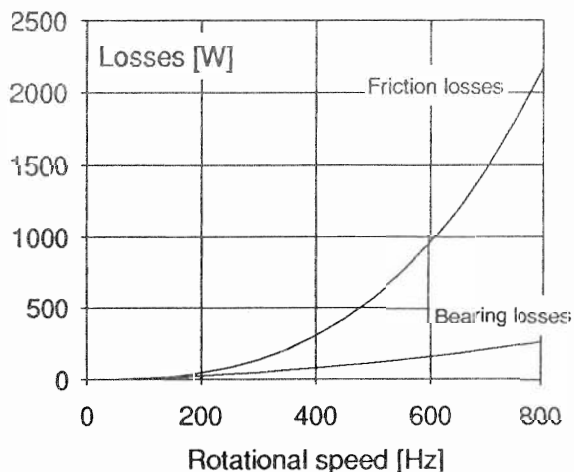


Fig. 10. Friction losses and active magnetic bearing losses.

the high-speed machines. The bearing losses are of minor importance in the compressor applications, but could be of major importance in other applications, such as vacuum applications. It must be remembered that the bearing losses are inside the rotor, so they are important considering the cooling of the rotor.

4 Conclusions

The successful design of the water treatment compressor is presented. In order to be able to design an efficient high-speed machine, powerful design tools are necessary for the electric motor and turbomachine as well as for the active magnetic bearings and rotor dynamics. The critical performance values of the electrical motor and active magnetic bearings have to be verified by measurements. In order to be able to start series production of machines with AMBs the most critical design factors have to be sorted and manufacturing tolerances have to be set.

References

- [1] Arkkio A. Analysis of induction motors based on the numerical solution of the magnetic field and circuit equations. Acta Polytechnica Scandinavia, Electrical Engineering Series 59, Helsinki 1987, Finland, p. 97.
- [2] Saari J. Thermal modelling of high-speed induction machines. Acta Polytechnica Scandinavia, Electrical Engineering Series 82, Helsinki 1995, Finland, p. 82.
- [3] Arkkio A., Lindgren O. 1994. "Finite Element Analysis of the Magnetic Forces Acting on an Eccentric Rotor of a High-Speed Induction Motor," Proceedings of the Fourth International Symposium on Magnetic Bearings, pp. 225-230, ETH Zürich, Switzerland.
- [4] Lantto E. 1994. "An Elastic Rotor Model for High-Speed Electrical Machines with Active Magnetic Bearings," Proceedings of the Fourth International Symposium on Magnetic Bearings, pp. 275-280, ETH Zürich, Switzerland.